Macroscopic self trapping in BECs: analysis of a dynamical quantum phase transition

B. Juliá-Díaz,[1] D. Dagnino,[1] M. Lewenstein,[2,3] J. Martorell,[1] and A. Polls[1]

[1] *Departament d'Estructura i Constituents de la Matèria, Universitat de Barcelona, 08028 Barcelona, Spain*

[2] *ICREA-Institució Catalana de Recerca i Estudis Avançats, Lluís Companys 23, 08010 Barcelona, Spain*

[3] *ICFO-Institut de Ciències Fotòniques, 08860 Castelldefels (Barcelona), Spain*

(Dated: May 13, 2010)

We consider a Bose-Einstein condensate in a double-well potential undergoing a dynamical transition from the regime of Josephson oscillations to the regime of self-trapping. We analyze the statistical properties of the ground state (or the highest excited state) of the Hamiltonian in these two regimes for attractive (repulsive) interactions. We demonstrate that it is impossible to describe the transition within the mean-field theory. In contrast, the transition proceeds through a strongly correlated delocalized state, with large quantum fluctuations, and spontaneous breaking of the symmetry.

PACS numbers: 03.75.Kk 03.75.Lm 74.50.+r

I. INTRODUCTION

Cold atom physics, e.g. Bose-Einstein condensates (BEC), provides a useful set up to tackle fundamental problems of quantum physics at a macroscopic scale. The physics of weakly interacting Bose gases has been described very successfully by employing a mean field approach, that is the Gross-Pitaevskii equation (GPE). Such approach implies that to a certain extent quantum fluctuations and correlations are relatively unimportant in a large variety of phenomena, see for instance [1].

A. Quantum correlations and symmetry breaking

The mean field approach can be improved by including in the theoretical description small (Gaussian) fluctuations around the mean field solutions. These fluctuations are described then by the Bogoliubov-de Gennes (BdG) equations, and have been intensively studied in experiments and theory [2]. The approach based on BdG equations has its limits also. In particular, it is completely inadequate in strongly correlated quantum systems, such as for instance those that can be realized with ultracold gases in optical lattices, or in low dimensional gases (for recent reviews see [3, 4]). Interestingly, it has recently been pointed out by several authors that the BdG approach breaks down in systems that undergo transition between two states that are well described by the mean field theory, but that differ dramatically in form, for instance having different symmetry properties. Transition between such states on the level of mean field description is typically associated with dynamical instabilities of the GPE, and exponential growth and squeezing of the BdG fluctuation. The state of the system in such situations becomes strongly correlated and entangled, and its description requires necessarily to go beyond the mean field theory. Several authors have pointed out this fact in various contexts: sonic analogues of "black holes" [5], vortex nucleation in small atomic clouds [6–9], BECs in rotating ring superlattices [10], or in the ground state of BEC in a double well potential [11].

Let us explain how the quantum correlations attain significance for the case of vortex nucleation in a rotating BEC [7]. In this paper exact diagonalization methods for small atomic clouds are used and compared with the mean field description, indicating directly the impossibility of a correct description of the transition within the mean field formalism. By performing the exact diagonalization of the Hamiltonian of the system, the authors show that in the transition region the atoms are far from being in the same single particle state. Instead, two macro-occupied single particle states (MSPS) appear with comparable occupations.

In this article we will show how the physics of BECs in a double-well resembles the above scenario. In the case of the rotating BEC, the control parameter driving the transition is the rotation frequency. In the case of the BEC in a double-well, it will be the interaction between the atoms, or, correspondingly, the height of the potential barrier splitting the BEC. Contrary to the previous works, that focus on the properties of the ground state, or low energy states of the considered system, we deal here with the dynamical transition both for attractive and repulsive interactions, for which also the properties of the highest energy, or high energy states are relevant.

B. BECs in double well potentials

The physics of BECs on a double-well has attracted a great deal of attention since the first theoretical studies predicting the presence not only of Josephson-like oscillations of population, but also of self-trapped states, see Refs. [12, 13]. Its recent experimental characterization by the Heidelberg group [14] opens the possibility of practical applications of these bosonic junctions.

As pointed out in Ref. [1], most of the physics of bosonic Josephson junctions, including self-trapping, $\pi-$modes and Josephson oscillations, can be understood

semiclassically. We will describe, however, how the transition from the Josephson-regime to the self-trapped regime is indeed dominated by quantum correlations. To that extent we will consider the exact diagonalization of the Bose-Hubbard (BH) Hamiltonian, and compare the results always to predictions of the semiclassical approach (in which quantum mechanical operators are replaced by their c-number averages).

Our aim is to isolate the purely quantum aspects of the transition, defined as those which are either not understandable in terms of a mean field description of the problem or, alternatively, by an elementary semiclassical analysis.

C. The plan of the paper

We will start, sections II-IV, discussing the properties of the BH Hamiltonian emphasizing the relevance of the condensed fractions, eigenvalues of the one-body density matrix, and the symmetry properties of the eigenstates of the Hamiltonian. By analyzing several quantities simultaneously we are able to classify the different regimes into which the transition is divided and which are clearly beyond the mean field approximation taken previously by some authors. The quantum nature of the transition is clearly visualized. Then, in section V, we present the dynamical consequences of the statical properties described before. The final section, VI, gives the conclusions of our analysis.

II. DESCRIPTION OF THE MODEL

As described in [1, 13] the two-mode Bose-Hubbard Hamiltonian for N atoms in the simple case of a double-well may be written as,

$$\begin{aligned} H &= \frac{-U}{2}\left(\hat{n}_L(\hat{n}_L-1)+\hat{n}_R(\hat{n}_R-1)\right) \\ &- J\left(a_R^\dagger a_L + a_L^\dagger a_R\right) - \epsilon(\hat{n}_L-\hat{n}_R) \end{aligned} \qquad (1)$$

where $a_L^\dagger|n_L,n_R\rangle=\sqrt{n_L+1}|n_L+1,n_R\rangle$, $a_L|n_L,n_R\rangle=\sqrt{n_L}|n_L-1,n_R\rangle$, and $[a_i^\dagger,a_j]=\delta_{i,j}\,,\quad i,j=L,R$. $L(R)$ stands for the left (right) side of the well. Our sign convention is such that $U>0(U<0)$ corresponds to attractive (repulsive) atom-atom interactions. We discuss both cases simultaneously as the technicalities are similar for both cases. We take $J>0$.

A small bias, $0<\epsilon\ll J$, is introduced which will ensure breaking of left-right symmetry. Numerically we consider, $\epsilon/J=10^{-10}$ in all the results presented, which intents to provide a realistic implementation of the symmetric double well.

The Hamiltonian is diagonalized in the $N+1$ dimensional space spanned by the basis: $\{|N,0\rangle,|N-1,1\rangle,\ldots,\ |1,N-1\rangle,|0,N\rangle\}$. With, $|n_L,n_R\rangle=1/\sqrt{n_L!n_R!}(a_L^\dagger)^{n_L}(a_R^\dagger)^{n_R}|\mathrm{vac}\rangle$. The dynamics of the system is governed by the ratio, $\Lambda\equiv NU/J$, which is controlled either by varying the atom-atom interactions U, or, by changing the barrier height, J.

Any single particle state may be written as, $|\Psi_1(\theta,\phi)\rangle=\cos(\theta/2)|L\rangle+e^{\imath\phi}\sin(\theta/2)|R\rangle$, a representation usually employed to describe single qubits [15]. We define, $|L(R)\rangle\equiv a_{L(R)}^\dagger|\mathrm{vac}\rangle$, and $|\pm>\equiv(1/\sqrt{2})(|L\rangle\pm|R\rangle)$.

The most general N-body state can be written as, $|\Psi\rangle=\sum_{k=1,N+1}c(k)|N+1-k,k-1\rangle$. The number of atoms in each well for a given state is, $N_\beta=\langle\Psi|a_\beta^\dagger a_\beta|\Psi\rangle$, with $\beta=L,R$. The population imbalance of a state Ψ is defined as, $z=(N_L-N_R)/N$. The time evolution of a state $\Psi(0)$ is governed by the time-dependent Schr̈odinger equation.

To characterize the degree of condensation of the system at any given time we will make use of the one-body density matrix, ρ. For a state, Ψ, we have, $\rho_{ij}=\langle\Psi|\hat{\rho}_{ij}|\Psi\rangle$, with $\hat{\rho}_{ij}=a_i^\dagger a_j$, and $i,j=L,R$. The trace of ρ is normalized to the total number of atoms, N. We will denote its two eigenvectors as $\psi_{1(2)}$ and its normalized eigenvalues (divided by the total number of atoms N) as $n_{1(2)}$, with $n_1\geq n_2\geq 0$. We always have, $n_1+n_2=1$. n_i will correspond to the condensed fraction in the macro-occupied state ψ_i [1].

A measure of the spread of the state in the Fock basis will be given by the function $S=-\sum_{k=1}^{N+1}|c(k)|^2\log(|c(k)|^2)$. S is positive definite and has a maximum value for the equally populated state, $c^2(k)=1/(N+1)$, and is zero for a maximally localized state, $c(k)=\delta_{k,k_0}$.

To clearly identify the region where the quantum fluctuations will play a major role we will always compare our numerical results to semiclassical predictions. The semiclassics of the problem may be obtained by replacing the creation and anhilation operators by c-numbers, $a_{L(R)}=\sqrt{n_{L(R)}}e^{\imath\varphi_{L(R)}}$. We can define the phase difference as, $\varphi=\varphi_R-\varphi_L$. The semiclassical Hamiltonian reads,

$$\frac{H}{NJ}=-\sqrt{1-z^2}\cos\varphi-\frac{\Lambda}{4N}(Nz^2+N-2)\,, \qquad (2)$$

and the time evolution of the population imbalance and phase difference is obtained through the Heisenberg evolution equations, $i\dot{a}_L=-[H,a_L]$ and $i\dot{a}_R=-[H,a_R]$. The resulting equations are, $\frac{\dot{z}(t)}{2J}=-\sqrt{1-z^2}\sin\varphi$, and $\frac{\dot{\varphi}(t)}{2J}=-\frac{\Lambda}{2}z+\frac{z}{\sqrt{1-z^2}}\cos\varphi$, which were originally obtained by Smerzi *et al.* [12] as the two-mode approxi-

[1] Other authors, e.g. Ref. [16, 17], introduce the operators, $J_x=(1/2)(a_L^\dagger a_R+a_R^\dagger a_L)$, $J_y=(1/2\imath)(a_L^\dagger a_R-a_R^\dagger a_L)$, and $J_z=(1/2)(a_L^\dagger a_L-a_R^\dagger a_R)$, which are related to ρ though, $\rho_{LL}=N/2+\langle J_z\rangle$, $\rho_{RR}=N/2-\langle J_z\rangle$, $\rho_{LR}=\langle J_x+\imath J_y\rangle$, and $\rho_{RL}=\langle J_x-\imath J_y\rangle$.

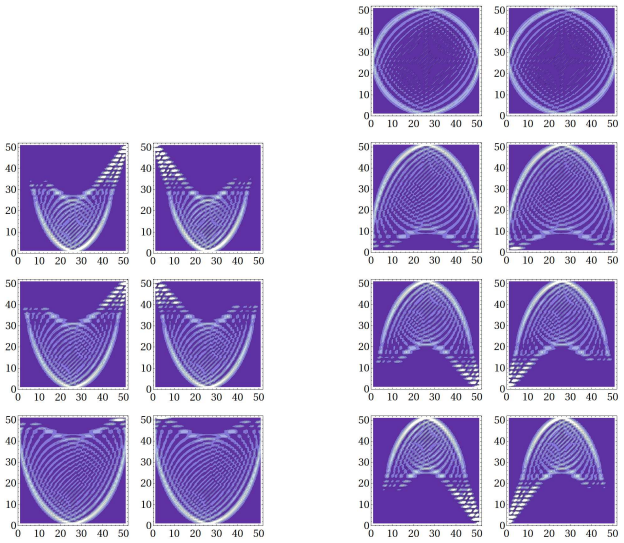

FIG. 1: Density plot of $|c_\lambda(k)|^2$, the horizontal (vertical) axes run through $k = 1, \ldots, N+1$ ($\lambda = 1, \ldots, N+1$), for, starting from above, (left) $NU/J = -4, -8, -12$ and (right) $NU/J = 0, 4, 8, 12$. The left (right) column of each two displays the eigenvectors with positive (negative) imbalance. Blue corresponds to zero and white to the maximum value. N is 50.

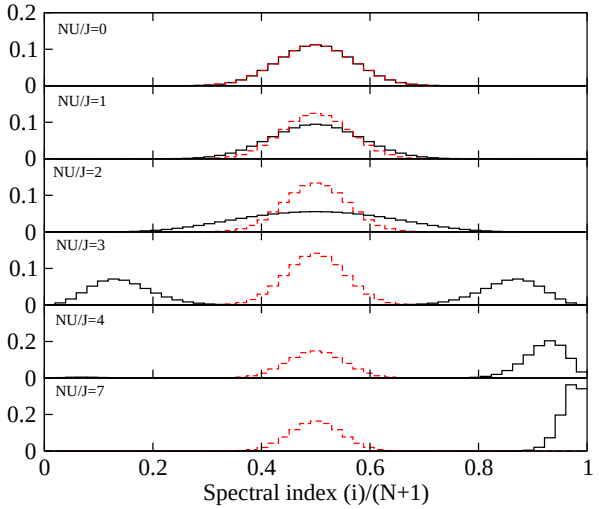

FIG. 2: Spectral decomposition, $|c_\lambda(k)|^2$ of the ground state (solid, black) and the highest state of the Hamiltonian (dashed, red) in the basis spanned by $(n_L, n_R) = \{(N,0), (N-1,1), \ldots, (0,N)\}$ for $N = 50$. If $U \to -U$ the same plots would be obtained, but with the roles of the ground and highest excited states exchanged.

mation to the Gross-Pitaevskii mean field description of the problem.

Ref. [12] defined the transition from the Josephson to the self-trapped regime as a dynamical feature, that is, a state initially prepared with a certain $(z(0), \varphi(0))$ would undergo Josephson oscillations or would remain self-trapped on one side of the double-well if Λ is larger than a critical value. We will link that definition, which is a semiclassical one in our model, with the static properties of the BH Hamiltonian.

III. GENERAL PROPERTIES OF THE SPECTRUM

Following the discussions of Refs. [16], let us first present the spectral decomposition, $|c_\lambda(k)|^2$, of the eigenvectors of the Hamiltonian, $H\Psi_\lambda = E_\lambda \Psi_\lambda$, as a function of Λ, see Fig. 1. Fig. 2 concentrates on the properties of the ground state and the highest excited state of the spectrum as we vary the value of $\Lambda = NU/J$. The main features relevant for our discussion are:

A. Attractive interactions: ground state analysis

When $\epsilon = 0$ the ground state is symmetric and binomial for the non-interacting case, $\Psi_{GS} = (1/\sqrt{N!})[(1/\sqrt{2})(a_L^\dagger + a_R^\dagger)]^N |\text{vac}\rangle$. Then, as the interaction is increased the ground state becomes wider. Then, it becomes degenerate with the next excited state, and its distribution has eventually two differentiated peaks, thus becoming cat-like [18]. When $\epsilon > 0$, but small, Figs. 1, and 2 show that, as we increase the interaction further, each of the formerly degenerate pairs develops a certain population imbalance and the distribution becomes peaked on only one region of the Fock space. It is important to note that the left-right symmetry is broken for a certain value of Λ, thus, the ground state will spontaneously acquire a large imbalance. Our figure differs from Fig. 2 of Ref [16], because we have artificially broken the symmetry with the help of a small bias. In this way the two degenerate eigenstates are distinguished according to their imbalance. Our figure emphasizes the symmetry breaking pattern, which occurs when the system evolves from cat-like to self-trapped.

B. Repulsive interactions: analysis of the highest energy state

The case of repulsive interactions is similar but the role played by the ground state is now played by the highest excited state of the Hamiltonian. With no interaction, the highest eigenvector of the Hamiltonian is also binomial, $\Psi_{\text{HE}} = 1/\sqrt{N!}[(1/\sqrt{2})(a_L^+ - a_R^+)]^N |\text{vac}\rangle$, as the interaction increases, undergoes similar features as the ground state did in the attractive case. The ground state in this case, on the contrary, remains mostly binomial with a certain squeezing, as also discussed in Ref. [19].

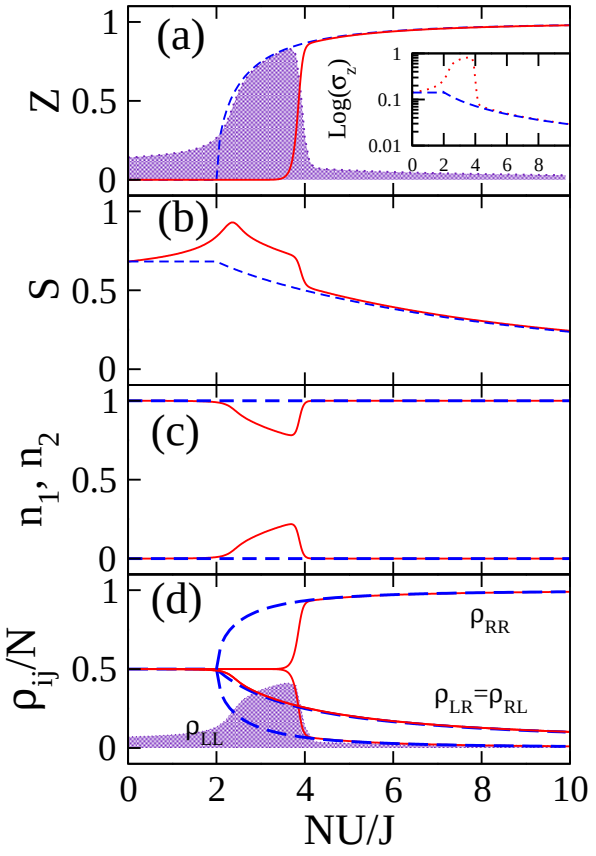

FIG. 3: (a) Solid line: population imbalance z of the ground state. The shaded region corresponds to its dispersion, σ_z. The inset provides a logarithmic view of σ_z, computed from the BH (dotted) and its semiclassical approximation (dashed). (b) A measure of the spread of the ground state, S, normalized to its maximum value, which would correspond to a equidistributed state. (c) Solid and dotted lines depict the condensed fractions, n_1 and n_2, of the one body density matrix of the ground state of the Hamiltonian, with imbalance ≥ 0 as a function of $\Lambda = NU/J$. (d) The four matrix elements of ρ are depicted as a function of NU/J. The shaded region corresponds to the variance of the diagonal elements, σ_{LL}, where $\sigma_{ij} \equiv \sqrt{|\langle\hat{\rho}_{ij}^2\rangle - \langle\hat{\rho}_{ij}\rangle^2|}$ (σ_{RR} turns out to be equal to σ_{LL}). The variance of the off-diagonal ones is negligible in this plot. The dashed lines in all the plots correspond to the semiclassical predictions (at $\epsilon = 0$): $z_{\rm s.c.} = 0$ if $\Lambda < 2$, $z_{\rm s.c.} = \sqrt{1 - 4/\Lambda^2}$ if $\Lambda \geq 2$. $\rho^{\rm s.c.}_{L,L} = N/2 + N z_{s.c.}/2$, $\rho^{\rm s.c.}_{R,R} = N/2 - N z_{s.c.}/2$, $\rho^{\rm s.c.}_{L,R} = \rho^{\rm s.c.}_{R,L} = N(\sqrt{1 - z^2_{\rm s.c.}})/2$. The number of atoms is, $N = 50$.

IV. ATTRACTIVE INTERACTIONS: QUANTUM FLUCTUATIONS

To characterize the problem more deeply, we now turn to other static properties of the eigenstates. In Fig. 3 we present several properties of the ground state as we increase the interaction, for the case of attractive interactions. The first magnitude is the population imbalance. As seen from the figure, it remains zero until a certain value (4 for $N = 50$) of Λ, then it grows abruptly and approaches 1 as Λ increases. The semiclassical approximation would predict such behavior to occur at $\Lambda = 2$. The discrepancy between the semiclassical prediction and the observed quantum behavior is diminished as the number of atoms, N, is increased. The figure also shows a shaded region corresponding to $\sigma_z \equiv \sqrt{\langle z^2\rangle - \langle z\rangle^2}$. In the region where the semiclassics fails, the dispersion of z becomes large. This agrees with the previous discussion of Figs. 1,and 2, and corresponds to the region where the ground state gets wider and, eventually, cat-like [2]. The authors of Ref. [20] consider the population imbalance as a suitable order parameter to characterize the transition.

The one body density matrix turns out to be a good indicator of where the semiclassics fails to describe the full quantum results. In the third panel we present the condensed fractions, n_1 and n_2, for different values of Λ. In the semiclassical limit, the system remains always fully condensed regardless of the value of Λ. This is clearly not the case in the transition region. For $N = 50$, the exact dynamics differs in the region $2 \lesssim \Lambda \lesssim 4$. In that region there are two MSPS, thus being impossible to describe the system within a mean field formalism. The macro-occupation can be traced back to the four elements of the one body density matrix, see panel (d). The off-diagonal ones are well described by the semiclassics in the whole considered domain, but the diagonal ones remain constant (=1/2) for $\Lambda \lesssim 4$. The dispersion of the diagonal matrix elements is directly related to σ_z, and is again large in the transition region. The dispersion of the off-diagonal elements is always of the order of 1% (thus explaining the agreement with the semiclassical picture).

The large quantum fluctuations seen in z, or ρ_{ii}, cannot be described in a mean field description. The inset in panel (a) of Fig. 3 shows σ_z computed assuming the state of the system corresponds to a mean-field state $\Psi_{\rm MF} = [|\Psi_1(\theta,\phi)\rangle]^{\otimes N}$, with θ, ϕ taken from their semiclassical values. As shown, both the full quantum result and the mean-field one agree at $\Lambda = 0$ and for $\Lambda \gtrsim 4$, but strongly disagree in the transition region. Finally, the spread of the state in the Fock basis, S, is presented in (b). The function has its maximum spread for $\Lambda \sim 2.4$, then falls and has an abrupt fall off when the ground state evolves from cat-like to self-trapped, $\Lambda \sim 4$.

The corresponding evolution of the two MSPS is given in fig. 4. There we plot in the $(|L\rangle, |R\rangle)$, $(|+\rangle, |-\rangle)$ plane their evolution as we increase the value of Λ. The exact results behave as follows: for $0 \lesssim \Lambda \lesssim 2$ the ground state of the system is fully condensed on the $|+\rangle$ state. It is thus symmetric, $z = 0$. For $2 < \Lambda \lesssim 3.5$ the same two single particle states are macro-occupied in the entire domain, see Fig. 3: $\psi_1 = |+\rangle$, and $\psi_2 = |-\rangle$. The system

[2] Employing the language of other authors, e.g. Ref. [16], we would have that for such region the semiclassical assumption does not hold, $\langle\{J_z, J_z\}\rangle \neq 2\langle J_z\rangle\langle J_z\rangle$.

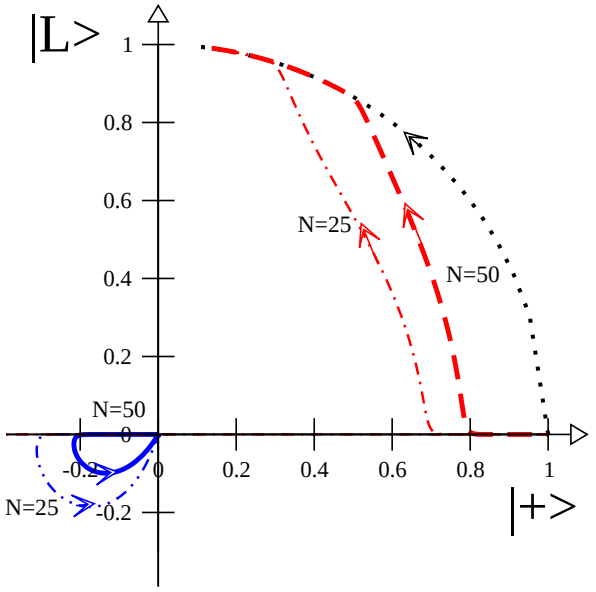

FIG. 4: Evolution of the MSPS of the ground state of the system as a function of Λ. The dashed and solid lines depict the BH calculation and correspond to ψ_1 and ψ_2, respectively. The MSPS are represented as $|\psi\rangle = \cos(\theta/2)|L\rangle + \sin(\theta/2)|R\rangle$. Their modulus is set to the condensed fraction of the state, n_i. The dotted line corresponds to the semiclassical prediction. All lines are obtained by evolving from $\Lambda = 0$, to 15. BH results are given for $N = 25$ and $N = 50$. (This figure corresponds to a vertical cut of the Bloch sphere used in Fig. 6.)

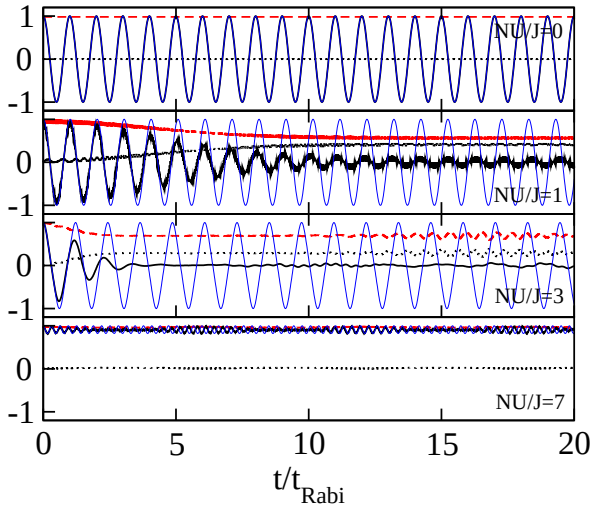

FIG. 5: Evolution of the population imbalance, thick-solid, and of the two macro-occupied condensed fractions, n_1 and n_2, dashed and dotted lines, as a function of time for a state initially prepared with $z(0) = 1$, $\Psi(0) = |N, 0\rangle$. The thin solid line corresponds to the semiclassical calculation of the population imbalance. The semiclassical values of n_1 and n_2 are the same for all panels and are constant and equal to 1 and 0, respectively. The panels correspond to different values of NU/J, in all cases with $N = 50$.

remains symmetric, $z = 0$. Their condensed fractions vary with Λ. For $3.5 \lesssim \Lambda \lesssim 4.5$ the system has still two MSPS but which depart from the $|\pm\rangle$ axis. These MSPS change continuously as we vary Λ, acquiring a non-zero z. Finally, for $\Lambda \gtrsim 4.5$ the system is fully condensed again, and ψ_1 approaches $|L\rangle$ as we increase Λ. The figure is constructed in such way that the departure from the semiclassical description becomes apparent immediately: any point outside of the circumference of radius one is beyond that appoximation. The dynamics is therefore mean-field like, both in the extreme Rabi regime, $NU/J \to 0$, and in the self-trapped regime, $NU/J \gtrsim 4.5$ for $N = 50$. The transition region cannot be described within a mean-field theory. The semiclassical approximation fails to describe the observed behavior almost in the entire domain of the transition.

The dependence of the described static properties as we vary N can be summarized as follows: increasing the number of atoms, the transition region gets reduced and thus the agreement with the semiclassical results, which predict a mean-field picture, is improved. As an example, Fig. 4 shows also the case of $N = 25$.

The dependence on the bias, ϵ is qualitatively similar: as ϵ is increased, the jump shifts to smaller values of Λ. In possible experimental set-ups it is however important to consider, as done in this work, ϵ which are almost negligible to ensure the transition region is broad enough in Λ.

V. DYNAMICS: THE GROUND AND THE HIGHEST ENERGY STATE

Up to now we have concentrated on describing the different phenomena occurring near the transition region by analyzing the static properties of the spectrum of the Hamiltonian as we varied the parameter Λ. Now we will consider the dynamical consequences. To this extent, we analyze the dynamics of the system with a fixed number of atoms, N, with a maximal initial population imbalance, $z(0) = 1$.

The simplest quantity which shows already quantum fluctuations is the population imbalance. In figure 5 the discrepancies between the semiclassical result and the exact solutions for the time evolution of the BH model are easily spotted. The BH model, with finite N, always brings in some damping to the oscillations, followed by revivals, in the Josephson regime [13]. The semiclassical results are seen to be accurate both for the case of no interaction among the atoms, Rabi oscillations, or the most self-trapped case. In the same figure we depict also the condensed fractions, n_1 and n_2. The semiclassical prediction for these quantities is always $n_1(t) = 1$ and $n_2(t) = 0$. In the finite N case however, we see how the condensed fractions do depart from 1 and 0, specially for the case $1 < NU/J \lesssim 4$.

In the case of attractive interactions the transition

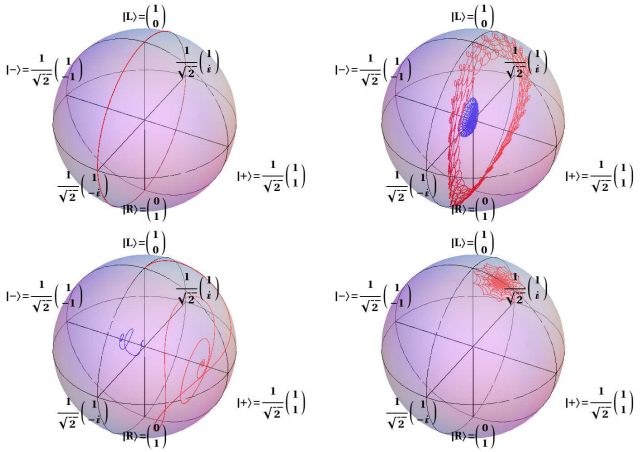

FIG. 6: 3D representation of the eigenvectors of the one body density matrix, $\psi_{1(2)}$ for $NU/J = 0, 1, 3, 7$ as a function of time. The total time is $5t_{\rm Rabi}$. The points are represented as follows: θ and ϕ are obtained from, $|\psi_{1(2)}\rangle = \cos(\theta/2)|L> + e^{\imath\phi}\sin(\theta/2)|R\rangle$. The distance to the origin is equal to $n_{1(2)}$. The initial state is always $z = 1$ with complete condensation on the $|L\rangle$ state. We mark also the $|\pm\rangle$ single particle states.

from Josephson to the self-trapped regime is completely related to the properties of the ground state of the system. Essentially, an initial state prepared with large imbalance and with Λ larger than a critical value will remain trapped due to its large overlap with the ground state of the system. Correspondingly, the self trapping for the case of repulsive interactions is directly related to the highest excited state of the Hamiltonian, which is the one with larger imbalance in this case.

In fig 6 we depict the time evolution of the two eigenvectors of ρ. The length of the eigenvector, ψ_i, in the Bloch sphere is set to its condensed fraction, n_i. Therefore, a fully condensed evolution will remain always on the surface of the sphere of radius 1. All other situations, involving two macroscopically occupied states, would fall inside the sphere.

The non-interacting case, $\Lambda = 0$, sets the Rabi oscillation time, $t_{\rm Rabi} = \pi/J$. The population imbalance performs periodic oscillations of maximum amplitude with the corresponding frequency, $\omega_{\rm Rabi} = 2J$. The system remains always condensed on a single particle state, see Fig. 6.

A small interaction, $NU/J = 1$, already changes the picture. First, in this case the system is no longer condensed at all times. Now, see second panel of fig 5 and the corresponding in fig. 6, as time increases the highest condensed fraction, n_1, goes from 1 to ~ 0.6 after $t > 10t_{\rm Rabi}$. The two MSPS rotate around the $(|+\rangle, |-\rangle)$ axis, and slowly approach the $|+\rangle$ and $|-\rangle$ states with a certain condensed fraction.

For $NU/J = 4$ self-trapping starts. The condensed fraction is large, ~ 0.9, but there are sizeable fluctuations. The behavior of the MSPS is now different, in this case they do not approach the $|+\rangle$ axis, but instead keep rotating around an axis closer to the $|L\rangle$ vector.

Larger interactions make the system more self-trapped and also to remain mostly condensed on a state progressively closer to $|L\rangle$. The size of the fluctuations seen in the condensed fractions decrease as we increase NU/J.

VI. CONCLUSIONS

We have scrutinized the transition from the Josephson to the self-trapped regime in BECs, for both attractive and repulsive atom-atom interactions. First, we have demonstrated the impossibility of a mean-field description of the quantum transition for a finite number of atoms, N, for attractive interactions. The nature of the transition, which involves the spontaneous breaking of the left-right symmetry, is governed by large quantum fluctuations which are not captured by a mean-field description of the problem. The ground state of the system in the transition is built of two macro-occupied single particle states. Both for attractive and repulsive interactions we have shown how the self-trapping regime is related to the existence of imbalanced eigenstates in the spectrum.

An extremely challenging experimental proposal emanates naturally from this article, namely, the full characterization of a quantum phase transition in a BEC, either by considering a varying barrier height in the double-well or by modifying the scattering length of the atom-atom interaction.

B.J-D. is supported by a CPAN CSD 2007-0042 contract. The authors thank D. Sprung for a careful reading of the manuscript and N. Barberán for discussions at early stages of the project. This work is also supported by Grants No. FIS2008-01661, FIS2008-00421, FIS2008-00784, FIS 2005-03169/04627 and QOIT from MEC/MINCIN, ESF/MEC project FERMIX (FIS2007-29996-E), EU Integrated Project SCALA, EU STREP project NAMEQUAM, ERC Advanced Grant QUAGATUA, and Alexander von Humboldt Foundation.

[1] A. J. Leggett, Rev. Mod. Phys. **73**, 307 (2001).
[2] L. Pitaevskii, and S. Stringari, *Bose-Einstein Condensation.* (Oxford University Press, Oxford, 2003).
[3] I. Bloch,, J. Dalibard, and W. Zwerger, Rev. Mod. Phys. 80, 885 (2008).
[4] M. Lewenstein, A. Sanpera, V. Ahufinger, B. Damski, A. Sen (De) and U. Sen, Advances in Physics 56, 243 (2007).
[5] L. J. Garay, J. R. Anglin, J. I. Cirac, and P. Zoller, Phys. Rev. Lett. **85**, 4643 (2000).
[6] M. Ueda, and T. Nakalima, Phys. Rev. **A73**, 043603 (2006).
[7] D. Dagnino, N. Barberán, M. Lewenstein, and J. Dal-

ibard, Nature Phys. 5, 431437 (2009).
[8] D. Dagnino, N. Barberán, M. Lewenstein, Phys. Rev. A 80, 053611 (2009).
[9] M. I. Parke, N. K. Wilkin, J.M.F. Gunn, and A. Bourne, Phys. Rev. Lett. **101**, 110401 (2008).
[10] A. Nunnenkamp, A. M. Rey, and K. Burnett, Phys. Rev. A **77**, 023622 (2008).
[11] C. Weiss, and N. Teichmann, Phys. Rev. Lett. **100**, 140408 (2008).
[12] A. Smerzi, S. Fantoni, S. Giovanazzi, and S. R. Shenoy, Phys. Rev. Lett. **79**, 4950 (1997).
[13] G.J. Milburn, J. Corney, E. M. Wright, and D. F. Walls, Phys. Rev. A **55**, 4318 (1997).
[14] M. Albiez, R. Gati, J. Flling, S. Hunsmann, M. Cristiani, and M. K. Oberthaler, Phys. Rev. Lett. **95**, 010402 (2005).
[15] M. A. Nielsen and I. L. Chuang, "Quantum Computation and Quantum Information", Cambridge University Press (2001).
[16] M. Jääskeläinen, and P. Meystre, Phys. Rev. A, **71**, 043603 (2005),
[17] M. Jääskeläinen, and P. Meystre, Phys. Rev. A **73**, 013602 (2006).
[18] J. I. Cirac, M. Lewenstein, K. Molmer, P. Zoller, Phys. Rev. A **57**, 1208 (1998).
[19] J. Javanaien, M. Yu. Ivanov, Phys. Rev. A **60**, 2351 (1999).
[20] P. Ziń, J. Chwedeńczuk, B. Oleś, K. Sacha and M. Trippenbach, Euro. Phys. Lett. **83** 64007 (2008).